

Andrzej DZIERWA  
Lidia GAŁDA  
Mirosław TUPAJ  
Kazimiera DUDEK

## INVESTIGATION OF WEAR RESISTANCE OF SELECTED MATERIALS AFTER SLIDE BURNISHING PROCESS

### BADANIA ODPORNOŚCI NA ZUŻYCIĘ WYBRANYCH MATERIAŁÓW PODDANYCH PROCESOWI NAGNIATANIA ŚLIZGOWEGO\*

*The article presents the research on the impact of slide burnishing process carried out with use of various ceramics on friction and wear of steel elements. In addition, surfaces after grinding, lapping and polishing processes were tested. The tribological couple was made of steel discs, toughened to a hardness of  $40 \pm 2$  HRC, and balls made of 100Cr6 steel with a hardness of 62 HRC. The tests were carried out at three sliding speeds: 0.16 m/s, 0.32 m/s and 0.48 m/s. The research proved the possibility of improving selected tribological properties of friction pairs thanks to the use of slide burnishing process and also allowed to establish a number of relationships between the parameters characterizing the surface topography and the tribological parameters.*

**Keywords:** surface topography, friction, wear.

*W artykule przedstawiono wyniki badań wpływu procesu nagniatania ślizgowego realizowanego z wykorzystaniem różnych ceramiki na wielkość zużycia oraz siłę tarcia elementów stalowych. Dodatkowo badaniom poddano powierzchnie po procesach szlifowania, docierania oraz polerowania. Skojarzenie materiałowe stanowiły tarcze stalowe ulepszone cieplnie do twardości  $40 \pm 2$  HRC oraz kulki ze stali 100Cr6 o twardości 62 HRC. Badania zrealizowano przy trzech prędkościach poślizgu: 0,16 m/s, 0,32 m/s oraz 0,48 m/s. Badania udowodniły możliwość poprawy wybranych właściwości tribologicznych par tarcznych dzięki zastosowaniu procesu nagniatania ślizgowego a także pozwoliły na ustalenie szeregu zależności pomiędzy parametrami charakteryzującymi strukturę geometryczną powierzchni oraz parametrami tribologicznymi.*

**Słowa kluczowe:** struktura geometryczna powierzchni, tarcie, zużycie.

#### List of abbreviations and symbols:

$F_{30}$  – value of the friction force obtained for the sliding distance equal to 30 m,  
 $F_{\text{sr}}$  – average value of the friction force,  
Hm – maximum values of the microhardness of the surface layer,  
 $\sigma_{\text{max}}$  – maximum values of residual stresses of the surface layer,  
Sal – fastest-decay autocorrelation length,  
Sk – core roughness depth,  
Sku – kurtosis,  
Spd – peak density,  
Spk – reduced peak height,  
Sq – root mean square height of the surface,  
Ssk – skewness,  
Svk – reduced valley depth,  
Sz – maximum height of the surface,  
VD – wear volume of the discs,

#### 1. Introduction

Any new technical object constructed in accordance with the requirements contained in the design and technological documentation has its own, full operational potential. During operation, and in the result of work performed this potential is decreased, in the result of the occurring physicochemical changes of elements, i.e. the wear of

friction pairs, material fatigue, corrosive processes, etc. [13]. These changes can reduce reliability, increase failure rate, or reduce object performance. Destruction processes occur in the result of working conditions, referred to as wear [36], which cause a sudden or gradual loss of performance of the elements. Because wear in most cases leads to a reduction in the operating potential of machines and their components it should be countered. This countermeasures should start at the design stage, with appropriate selection of elements of the tribomechanical assembly, so as to reduce wear during operation. In addition to design, a number of technological methods of wear prevention are also applied. These can include, among others, the following [1, 4, 38]:

- use of heat and thermo-chemical treatment (e.g. harden nitriding, carburizing, cyaniding),
- use of plastic forming of metals (e.g. hammering, burnishing),
- applying overlays and coatings (e.g. chemical nickel plating, hard facing).

Burnishing is one of the surface treatments that can delay wear processes [22]. It includes ways such as roller burnishing [11], roller finishing, slide burnishing [17] and even similar techniques like shot-peening [9, 16]. In the case of slide burnishing, a hard and smooth burnishing element is pressed against the machined surface with the appropriate force, causing sliding friction in the burnishing zone and, as in the consequence of this process, smoothing of the surface and beneficial changes in the properties of the surface layer of the object

(\*) Tekst artykułu w polskiej wersji językowej dostępny w elektronicznym wydaniu kwartalnika na stronie [www.ein.org.pl](http://www.ein.org.pl)

[31]. By using slide burnishing, we can improve hardness of the [28, 33], attain good surface smoothness [14, 25, 30], form compressive stresses in the top layer [2, 32] and obtain a top layer free of abrasive contaminants. These features favorably affect a number of functional properties, including the tribological wear [5, 24], fatigue strength [33, 34] and corrosion resistance [28, 37].

In [6] the authors conducted tests of burnishing 6061 series aluminium alloy. They proved that by using appropriate machining parameters, it is possible to reduce the friction coefficient of friction couples by 48% and weight loss by 60-80%. Hamadache et al. [10] applied the burnishing process to Rb40 steel. The tests have demonstrated the severalfold increase in wear resistance, compared to samples after machining processes. The results of the research carried out by the authors of [18] demonstrate the beneficial effect of burnishing on the reduction of the friction coefficient and the wear of polymers in relation to the non-burnished samples. Polyurethane and polyformaldehyde were tested. The reduction of the friction coefficient in tribological tests for both polymers reached a maximum of 32%, while the wear was reduced by a maximum of 38%, when compared to samples subjected to machining processes. The degree of reduction of both the friction coefficient and the wear depended strongly on the initial value of the surface roughness. Revankar et al. [26] studied the tribological properties of the Ti-6Al-4V titanium alloy. They tested surfaces following the machining and burnishing processes, for a range of initial process input parameters. It was proved that for the most favorable parameters there was a 52% reduction in wear and a 64% reduction in friction coefficient compared to machined samples. Whereas the authors of [24] examined the wear resistance of two-phase HSLA steel alloys subjected to burnishing process. It was observed that a greater reduction in wear was recorded in the case of samples burnished with a greater load. The purpose of the work [35] was to determine the possibilities of limiting 316L steel damage caused by impact wear without disturbing the material structure. Burnishing was selected as the finishing treatment of the steel surface. Studies have demonstrated a 53-62% reduction in wear traces compared to the non-burnished samples. Janczewski et al. [12] studied low density and high molecular weight (LDPE) polyethylene samples. Milling and burnishing processes were selected as the finish. Burnishing proved to modify the LDPE surface and dramatically reduce wear by approx. 58% compared to milled samples.

During the studies on the influence of burnishing on the tribological properties of friction couples, in their vast majority, diamond or diamond composite is used as the burnishing element, which makes it a relatively expensive solution. There is little mention of the use of cheaper burnishing elements applied in particular to numerically controlled machine tools to improve these properties. The possibility of wider application of ceramic materials [3, 26] for their improvement would undoubtedly lead to a reduction of costs associated with the burnishing process, in particular in the case of obtaining surface quality at a level similar to that obtained as a result of using diamond tooling. It would, at the same time, eliminate or reduce labor-intensive finishing operations such as honing, grinding, polishing or superfinishing.

The present work presents the research on the impact of burnishing process carried out with use of various ceramics on selected tribological properties of steel - steel couples. In addition, our comparative analysis included standard machining processes used in machine construction, such as polishing, grinding and lapping.

## 2. Experimental

Tribological tests were carried out on a T-11 pin/ball - disc tribological tester, in the ball - disc configuration. The tribological couple was a stationary ball bearing with a hardness of

62±2 HRC and a disc made of 42CrMo4 steel with a hardness of 40±2 HRC. The finishing treatment of the discs consisted of burnishing processes completed with various types of ceramic balls ( $Al_2O_3$ , SiC, WC). Burnishing was performed using a vertical Hass VF-3 machining center using 3 different pressure forces of the tool: 30, 70 and 100 N. A single tool pass was used at a constant feed rate of 0.05 mm. In addition, discs in which grinding, polishing and lapping processes were the finishing treatment were tested. Isometric views of the surfaces of selected discs are presented in Fig. 1. In turn, Table 1 summarizes selected parameters of the surface topography of the tested discs [20]. For discs after the burnishing process the following designations were used:

- $Al_{30}$ ,  $Al_{70}$  and  $Al_{100}$  when the burnishing element was  $Al_2O_3$  ceramics (indexes denote the pressure force applied during burnishing),
- $SiC_{30}$ ,  $SiC_{70}$ ,  $SiC_{100}$  when the burnishing element was SiC ceramics,
- $WC_{30}$ ,  $WC_{70}$ ,  $WC_{100}$  when the burnishing element was WC ceramics.

In addition, the grinding, polishing and lapping processes were designated 'SZ', 'POL' and 'DOC' respectively. The sliding distance in all variants was 282.6 m, which corresponded to 30 minutes of the test. The tests were carried out at a load of 9.81 N and at three sliding speeds: 0.16; 0.32 and 0.48 m/s. During the tests, the friction force was measured, while after the tests the amount of wear was determined using a Talysurf CCI Light white light interferometer. Measurements of wear were made at four positions 90° apart, obtaining areas of 3.3 mm x 3.3 mm. Then, profiles were generated perpendicular to the wear track and the area of wear was calculated using TalyMap Gold 6.0 software. The next step was to calculate the volumetric wear of discs according to the formula (1):

$$VD = \pi dS \left[ m^3 \right] \quad (1)$$

where:

d – diameter of the wear track [mm],

S – cross-sectional area of the wear track [mm<sup>2</sup>].

All tests were repeated at least 3 times. Residual stress measurements were carried out with use of a portable Xstress 3000 G3R X-ray diffractometer. The measurements used the  $\sin 2\psi$  method [7] during which the angle of incidence  $\psi$  was in the range of -45° to +45°, divided into 7 tilt positions. Exposure time was set to 40 s. The X-ray

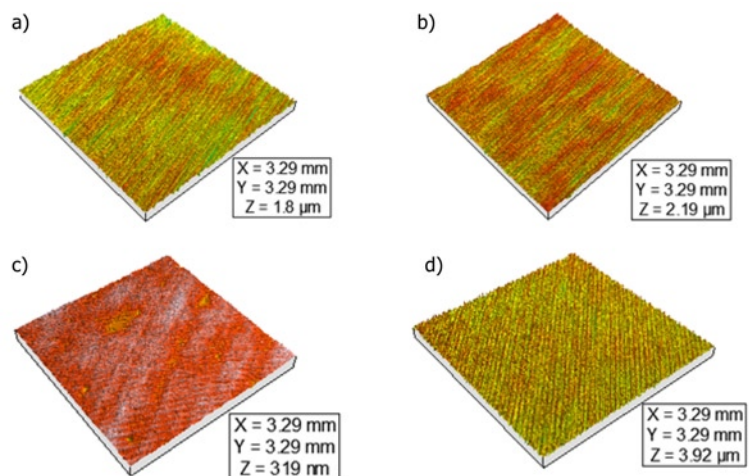


Fig. 1. Isometric views of selected discs: a) burnished sample  $Al_{70}$ , b) burnished sample  $SiC_{70}$ , c) polished sample, d) ground sample

Table 1. Selected surface topography parameters of tested discs

	Sq	Ssk	Sku	Sz	Sal	Spd	Sk	Spk	Svk
Al <sub>30</sub>	0.28	-0.898	4.36	2.84	0.0256	750	0.527	0.131	0.461
Al <sub>70</sub>	0.142	-1.24	6.12	1.8	0.0172	612	0.336	0.1741	0.325
Al <sub>100</sub>	0.186	-1.116	4.98	2.44	0.0185	672	0.426	0.148	0.389
SiC <sub>30</sub>	0.227	-1.07	5.14	2.56	0.214	304	0.385	0.1335	0.395
SiC <sub>70</sub>	0.117	-0.801	4.71	2.19	0.115	493	0.222	0.0538	0.17
SiC <sub>100</sub>	0.192	-0.569	3.89	1.98	0.166	468	0.351	0.0944	0.301
WC <sub>30</sub>	0.207	-0.951	5.9	3.76	0.0107	790	0.445	0.144	0.35
WC <sub>70</sub>	0.3	-0.321	3.86	3.46	0.379	574	0.465	0.119	0.387
WC <sub>100</sub>	0.226	-0.869	4.11	2.86	0.189	687	0.458	0.123	0.379
SZ	0.258	-0.277	3.81	3.92	0.0086	843	0.603	0.123	0.333
POL	0.0189	-0.17	2.9	0.319	0.214	1170	0.0319	0.01	0.0181
DOC	0.094	-0.59	4.39	1.3	0.0264	1020	0.198	0.0608	0.137

penetration depth was set to 10 μm and the XTronic software was used to compute the residual stresses. For each sample, residual stress was determined in 2 directions perpendicular and parallel to machining traces.

Microhardness measurements were carried out on a Brivisor KL2 microhardness tester with HME measuring electronics by means of static indenter induction using the Vickers method, with a constant load of P = 4.9 N. The impact time of the pyramid indenter with quadrilateral base with a double-wall angle of 136° was ca. 15 s. Surface microhardness of the examined samples was measured on microsections made at an angle of 5°.

### 3. Results and discussion

Figures 2-4 present the results of the tests. One by one the average values of volumetric wear of the tested disc surfaces for all sliding speeds (Fig. 2), the average values of the friction force obtained after the running-in process (Fig. 3) and the values of the friction force obtained for the sliding distance equal to 30 m (Fig. 4) are presented. Table 2 presents the maximum values of residual stress  $\sigma_{max}$  and microhardness Hm as well as confidence intervals  $u(\sigma_{max})$ ,  $u(Hm)$  of all samples subjected to tribological tests. Figure 5 shows the cross-sectional areas of wear of selected discs (Al<sub>70</sub> and POL), and Figure 6 shows examples of friction force curves for these frictional pairs at a sliding speed of 0.16 m/s.

At the lowest sliding speed of  $v = 0.16$  m/s, the largest volumetric wear was observed for the frictional pair with the polished disc. In this case the value of VD parameter was 0.694 mm<sup>3</sup> and corresponded to the highest value of the friction force obtained for the sliding distance equal to 30 m (7.522 N) and the highest average value of the friction force  $F_{sr}$  (8.308 N). The smallest value of VD parameter at the sliding

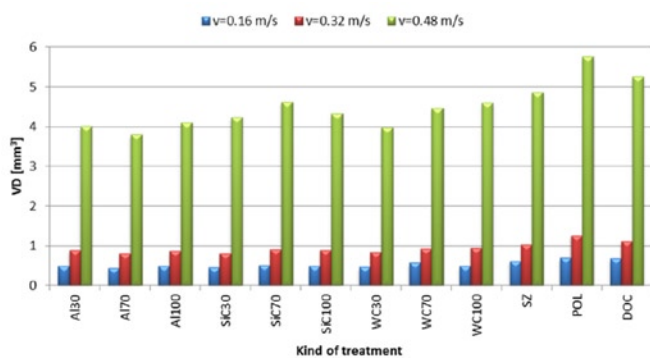


Fig. 2. Volumetric wear of disc sample

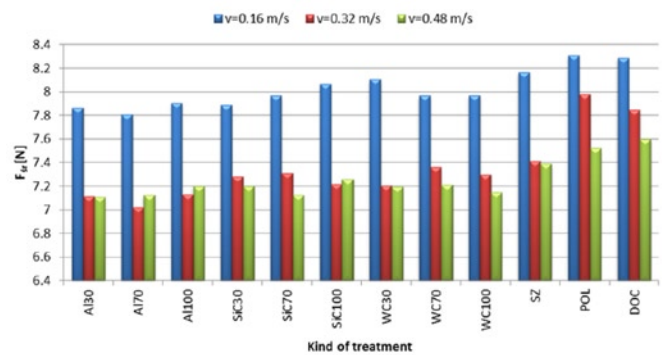


Fig. 3. Average friction force of disc samples

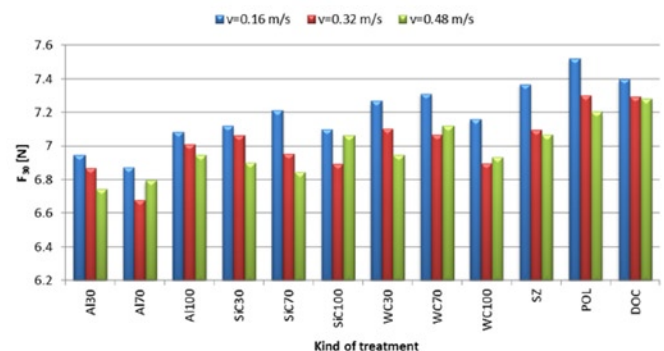


Fig. 4. Friction force of disc samples obtained for the sliding distance equal to 30 m

speed of  $v = 0.16$  m/s was calculated for the burnished sample Al<sub>70</sub> and it was 0.439 mm<sup>3</sup>. For this sample, the lowest average friction force  $F_{sr}$  was also observed, and it was 7.808 N. The friction coefficient  $\mu$  ranged from 0.79 (Al<sub>70</sub> sample) to 0.85 (polished sample).

An increase in the sliding speed to 0.32 m/s caused an increase in the value of volumetric wear of most samples and a slight decrease in the average value of the friction force and the value of the friction force obtained for the sliding distance equal to 30 m. Similar to the lowest sliding speed, the sample Al<sub>70</sub> had the lowest value of wear volume and it was 0.796 mm<sup>3</sup>. In the case of Al<sub>70</sub> sample the average value of friction force  $F_{sr}$  and  $F_{30}$  parameter were also the smallest – 7.022 N and 6.677 N respectively. The highest values of measured parameters were obtained for the polished sample. The VD parameter for this sample achieved 1.262 mm<sup>3</sup>. The friction coefficient  $\mu$  de-

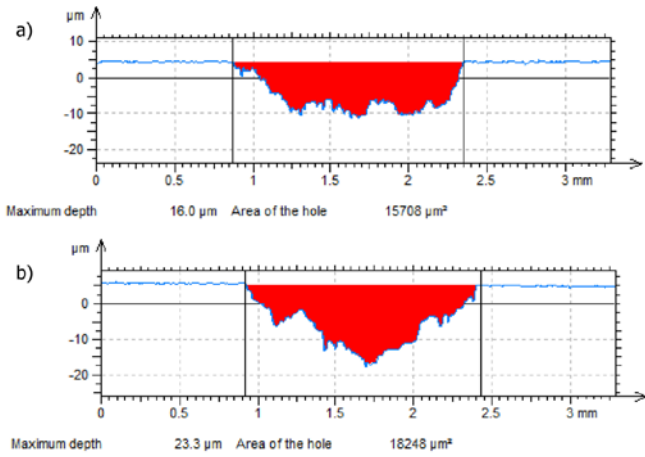


Fig. 5 Cross-sectional areas of worn discs: Al<sub>70</sub> (a) and POL (b) at the sliding speed of 0.16 m/s,

creased in comparison to the lowest sliding speed and ranged from 0.72 (Al<sub>70</sub> disc) to 0.81 (polished disc).

An increase in sliding speed to 0.48 m/s caused a very substantial

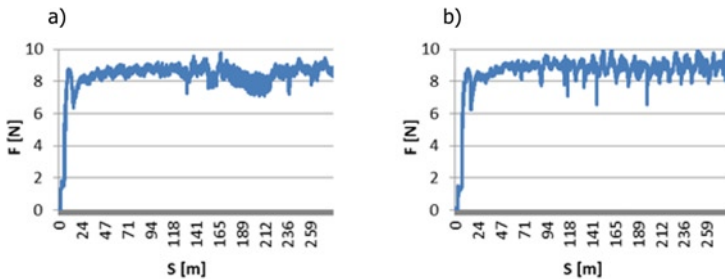


Fig. 6. Friction force versus sliding distance for selected worn discs Al<sub>70</sub> (a) oraz POL (b) at a sliding speed of 0.16 m/s

increase in the volumetric wear of all samples compared to the wear observed at lower sliding speeds. Al<sub>70</sub> sample was again characterized by the lowest wear volume at this sliding speed, however the lowest values of  $F_{sr}$  and  $F_{30}$  were observed for the sample Al<sub>30</sub>. The VD parameter of the Al<sub>70</sub> sample was 3.796 mm<sup>3</sup>. The highest value of volumetric wear was again measured for the polished sample and it was 5.759 mm<sup>3</sup>. In turn, the highest values of the  $F_{sr}$  and  $F_{30}$  parameters were recorded for the lapped sample and it was 7.598 N and 7.284 N, respectively. The lower value of the friction coefficient was at a similar level as at the sliding speed of 0.32 m/s, while the upper value slightly decreased compared to this speed. The friction coefficient was in the range of 0.72 (Al<sub>30</sub> sample) to 0.77 (lapped sample).

The highest values of maximum compressive stresses were obtained for the burnished samples SiC<sub>100</sub> and WC<sub>100</sub>. The measured values of these discs were -376.1 MPa and -349.6 MPa respectively. In turn, the highest maximum value of surface microhardness was observed for the burnished surface topography Al<sub>100</sub>. Despite this, mentioned samples were characterized by relatively high volumetric wear of the discs among the samples subjected to the slide burnishing process. The lowest values of the VD parameter were observed for Al<sub>70</sub> and SiC<sub>30</sub> discs at the sliding speed of 0.16 m/s, again for Al<sub>70</sub> and SiC<sub>30</sub> discs at the sliding speed of 0.32 m/s, as well as for Al<sub>70</sub> and WC<sub>30</sub> discs at the sliding speed of 0.48 m/s.

Table 2. Maximum values of residual stress  $\sigma_{max}$  and microhardness Hm of the surface layer

Sample	$\sigma_{max}$ [MPa]	$u(\sigma_{max})$ [MPa]	Hm [HV]	$u(Hm)$ [HV]
Al <sub>30</sub>	-212.6	±18.6	380.1	±11.6
Al <sub>70</sub>	-298.1	±17.8	389.4	±14.2
Al <sub>100</sub>	-309.8	±26.2	404.2	±14.8
SiC <sub>30</sub>	-270.3	±18.6	399.6	±13.4
SiC <sub>70</sub>	-301.6	±24.8	388.2	±11.6
SiC <sub>100</sub>	-376.1	±28.6	399.7	±12.2
WC <sub>30</sub>	-288.7	±26.1	382.4	±13.9
WC <sub>70</sub>	-344.6	±28.7	403.5	±12.2
WC <sub>100</sub>	-349.4	±24.4	398.8	±11.4
SZ	-37.2	±8.7	381.4	±12.2
POL	-179.2	±12.4	385.2	±14.6
DOC	-96.8	±10.2	384.1	±13.8

To illustrate the wear mechanism of worn surfaces, a surface topography analysis and scanning microscope (Vega3) analysis were performed. Surface topography analysis showed the formation of a one-directional texture after tribological tests. The values of Str (texture aspect ratio of the surface) were in the range of 6.98–13.06% and they were characteristic for anisotropic surfaces after abrasive wear. Figure 7 shows isometric views of Al<sub>70</sub> and POL discs after tribological tests, as well as slices of their worn surfaces. For the Al<sub>70</sub> sample the Str parameter equaled to 8.44%, and for the polished sample it was 9.13%.

Also, SEM analysis (Figure 8) confirms abrasion as the dominant wear mechanism. As a result, a complete change in the surface topography was observed. The tracks of wear on the disc surfaces include elongated craters in the sliding direction, and smoothed areas with longitudinal grooves resulting from plastic deformation. The presence of delaminations on the worn surface of discs was also observed.

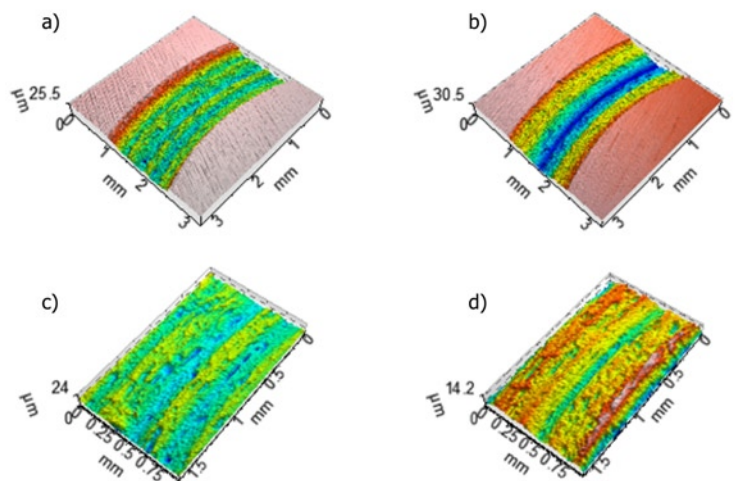


Fig. 7. Isometric views of the discs Al<sub>70</sub> (a) and POL (b) after tribological tests and details of their worn surfaces Al<sub>70</sub> (c) i POL (d)

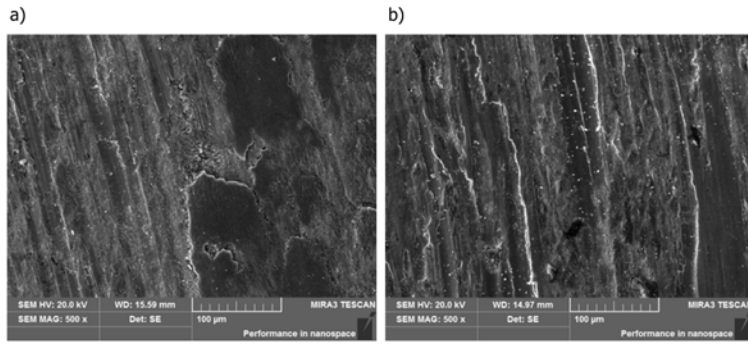


Fig. 8. Worn surfaces of the discs Al<sub>70</sub> (a) and POL (b) at the sliding speed of  $v = 0.16$  m/s

The coefficient of the linear correlation R was used to search for dependency between tribological parameters and parameters characterizing the surface topography. The value of the correlation coefficient ranges from -1 to 1. The higher its absolute value, the stronger the linear relationship between the variables. The value  $R = 1$  or  $R = -1$  indicates the complete linear dependency between the features, while  $R = 0$  indicates lack of such relation. A strong linear dependency occurring at all sliding speeds was found for VD-Ssk (skewness) and VD-Sku (kurtosis) pairs. These dependencies are shown in Figure 9. The skewness Ssk, also known as the asymmetry coefficient, characterizes the symmetry of the ordinate distribution of the roughness height relative to the mean plane [15]. According to [27], a negative value of this factor indicates a plateau like surface, while a positive one indicates the predominance of peaks. All tested discs were characterized by a negative value of the Ssk parameter, which ranged from -0.17 (polished disc) to -1.24 (Al<sub>70</sub> disc). In turn, the Sku parameter is determined by the measure of the peaks or sharpness of the surface height distribution. For the normal distribution of the ordinates  $Sku = 3$  [8]. Samples subjected to tribological tests were characterized by normal ordinate distribution or close to normal one. In

the case of volumetric wear of discs and the Ssk parameter, the coefficient of linear correlation R ranged from 0.77 (for  $v = 0.48$  m/s) to 0.83 (for  $v = 0.16$  m/s), and for VD and Sku parameter the coefficient of linear correlation R achieved values between -0.72 (for  $v = 0.16$  m/s) and -0.78 (for  $v = 0.32$  m/s) and it was inversely proportional. The smallest values of volumetric wear of discs were achieved for the minimum values of the Ssk parameter and the maximum values of the Sku parameter. Negative skewness can improve contact conditions by reducing the plasticity index, what can speed up the reduction in wear volume. Surfaces with a low value of Ssk and a high value of Sku can be „traps” for wear particles. In the case of the research in dry friction conditions and at ambient temperatures, wear particles typically have from about 10 to 100 µm. It seems that some of the particles were so small that the valleys of surface

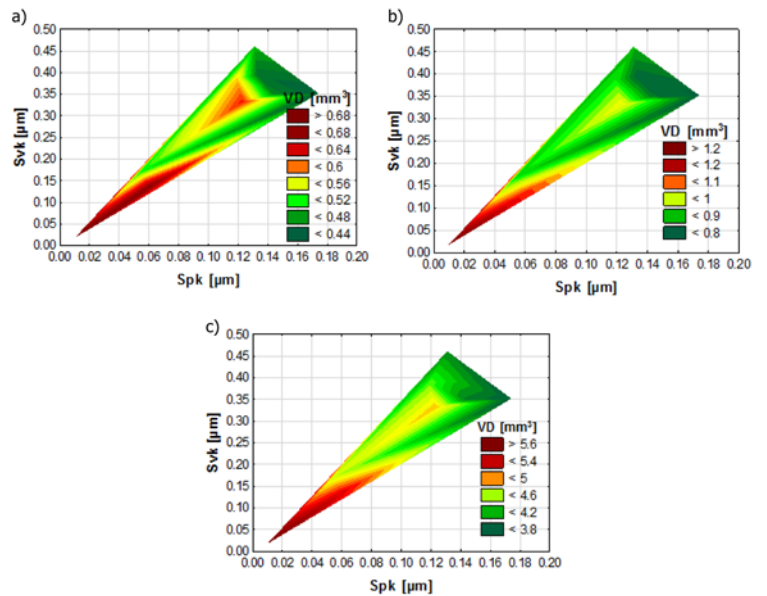


Fig. 10. Dependencies between wear volume VD and Spk i Svk parameters at the sliding speed of:  $v = 0.16$  m/s (a),  $v = 0.32$  m/s (b),  $v = 0.48$  m/s (c)

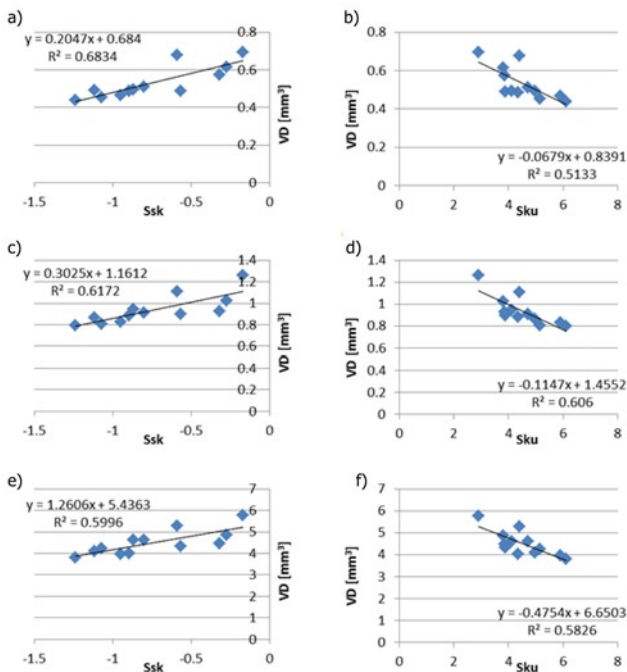


Fig. 9. Dependencies between wear volume VD and Ssk (a, c, e) and Sku (b, d, f) parameters at the sliding speed of: a, b)  $v = 0.16$  m/s; c, d)  $v = 0.32$  m/s; e, f)  $v = 0.48$  m/s

topography acted as traps for some of the wear products and helped to reduce the wear intensity. The situation could be different in the case of tests at elevated temperature, and comprehensive studies on the structure of wear products resulting from the friction process were conducted by the authors [39, 40].

A strong linear dependency occurring at all sliding speeds was also found for volumetric wear and parameters characterizing the Abbott-Firestone curve: Spk (reduced peak height), Svk (reduced valley depth) and Sk (core roughness depth). The relations between Spk and Svk are presented in Fig. 10. The areas marked in red indicate a higher value of the VD parameter, and the green one (in particular dark green) with less wear of the discs. Analyzing the obtained results, it can be seen that the increase in the Spk and Svk parameters corresponded to a decrease in the wear volume of the discs. The Svk parameter allows the evaluation of the lubricating properties of surfaces and is a measure of the ability to maintain fluid through the mating surfaces. In turn, higher values of the Spk parameter characterize surfaces with high peaks, which makes the area of initial contact relatively small and the force applied per unit of surface large. Therefore, the Spk parameter may represent the nominal height of the material that will be removed at the initial stage of the operation - running in [19]. An increase of Spk parameter leads to a reduction in the real contact surface, which may limit the impact of adhesive effects. The authors of [29] suggest that the Spk/Svk ratio is more important than the value

of these parameters separately. In all examined surface topographies, the  $S_{vk}$  parameter was greater than  $S_{pk}$ , which made the tribological couples tend to reduce the coefficient of friction (especially with a negative value of the  $S_{sk}$  parameter). The dependency between the  $S_k$  parameter and the wear volume of the discs seem to be particularly important. The  $S_k$  parameter controls the tribological properties of the elements after the running-in period. In the case of discs with a small roughness height this is particularly important because the running-in period in all tested configurations did not exceed 5 minutes. Therefore, this parameter can be taken into account when planning the surface topography with the desired tribological properties.

A strong dependency was also observed between volumetric wear and the  $S_{pd}$  parameter (peak density). This parameter determines the number of peaks by the unit area. The greater the value of the  $S_{pd}$  parameter, the greater the bearing surface [23], especially when the  $S_{sk}$  parameter is negative.

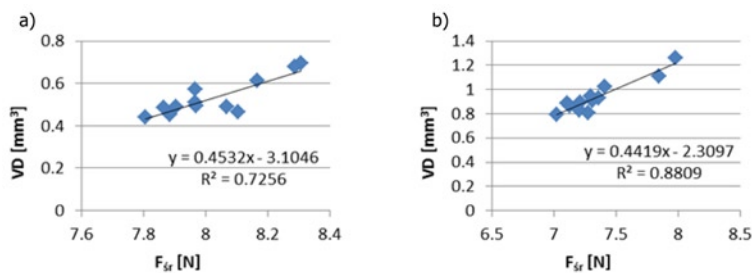


Fig. 11. Dependencies between wear volume  $VD$  and average value of friction force  $F_{fr}$  at the sliding speed of:  $v = 0.16$  m/s (a) and  $v = 0.32$  m/s (b)

The volumetric wear of the discs and the average value of the friction force were also characterized by a strong linear dependency (Fig. 11). Depending on the sliding speed, the coefficient of linear correlation was:  $R = 0.85$  at  $v = 0.16$  m/s;  $R = 0.94$  at  $v = 0.32$  m/s and  $R = 0.84$  at  $v = 0.48$  m/s. Also the values of friction force obtained for the sliding distance equal to 30 m were strongly correlated with the wear volume of the discs. In this case, depending on the sliding speed, the coefficient of linear correlation between  $VD$  and  $F_{30}$  achieved:  $R = 0.85$  at  $v = 0.16$  m/s;  $R = 0.73$  at  $v = 0.32$  m/s and  $R = 0.78$  at  $v = 0.48$  m/s. In turn, the wear volume of discs was not significantly correlated with the maximum value of residual stresses (coefficient of linear correlation ranged from  $-0.54$  to  $-0.64$ ) and microhardness (coefficient of linear correlation in the range:  $-0.25$  ÷  $-0.34$ ).

#### 4. Conclusions

Based on the tests carried out, we can conclude that the increase in sliding speed led to an increase in the wear volume of discs subjected to tribological tests. Of all samples, the lowest values of the  $VD$  parameter were recorded in the case of  $Al_{70}$  or  $SiC_{30}$  burnished discs. The wear volume of the discs was correlated with the average value of the friction force and also with the value of the friction force obtained for the sliding distance equal to 30 m.

A number of relationships between the parameters characterizing surface topography of the discs and wear volume were also found. A strong linear relationship was observed for the parameters characterizing the Abbot-Firestone curve ( $S_k$ ,  $S_{vk}$ ,  $S_{pk}$ ) as well as for the skewness and kurtosis of the surfaces ( $S_{sk}$  and  $S_{ku}$ ).

The tests proved the beneficial effect of the slide burnishing process (regardless of the ceramics applied) on the reduction of volumetric wear in friction pairs compared to other popular finishing treatments used in machine construction.

#### References

1. Bara M, Skoneczny W, Kaptacz S. A Tribological properties of ceramic-carbon surface layers obtained in electrolytes with a different graphite content. *Eksplotacja i Niezawodność - Maintenance and Reliability* 2008; 4: 66-70.
2. Chomienne V, Valiorgue F, Rech J, Verdu C. Influence of ball burnishing on residual stress profile of a 15-5PH stainless steel. *CIRP Journal of Manufacturing Science and Technology* 2016; 13: 90-96, <https://doi.org/10.1016/j.cirpj.2015.12.003>.
3. Dzierwa A, Markopoulos A P. Influence of ball-burnishing process on surface topography parameters and tribological properties of hardened steel. *Machines* 2019; 7(1): 11, <https://doi.org/10.3390/machines7010011>.
4. Dzierwa A, Pawlus P, Reizer R. The effect of ceramic tribo-elements on friction and wear of smooth steel surfaces. *Proceedings of the Institution of Mechanical Engineers, Part J: Journal of Engineering Tribology* 2019; 233(3): 456-465, <https://doi.org/10.1177/1350650118780779>.
5. El-Tayeb N S M. Frictional behaviour of burnished copper surfaces under dry contact conditions. *Engineering Research Bulletin* 1994; HU Cairo: 171-184.
6. El-Tayeb N S M, Low K O, Brevern P V. Enhancement of surface quality and tribological properties using ball burnishing process. *Machining Science and Technology* 2008; 12: 234-248, <https://doi.org/10.1080/10910340802067536>.
7. Fitzpatric M E, Fry A T, Holdway P, Kandil F A, Shackleton J, Suominen L L. Determination of Residual Stresses by X-ray Diffraction - Issue 2. A National Measurement Good Practice Guide No. 52: National Physical Laboratory, 2005.
8. Gademawla E S, Koura M M, Maksoud T M A, Elewa I M, Soliman H H. Roughness parameters. *Journal of Materials Processing Technology* 2002; 123: 133-145, [https://doi.org/10.1016/S0924-0136\(02\)00060-2](https://doi.org/10.1016/S0924-0136(02)00060-2).
9. Ganesh B K C, Sha W, Ramanaiah N, Krishnaiah A. Effect of shot peening on sliding wear and tensile behavior of titanium implant alloys. *Materials & Design* 2014; 56: 480-486, <https://doi.org/10.1016/j.matdes.2013.11.052>.
10. Hamadache H, Laouar L, Zeghib N E, Chaoui K. Characteristics of Rb40 steel superficial layer under ball and roller burnishing. *Journal of Materials Processing Technology* 2006; 180: 130-136, <https://doi.org/10.1016/j.jmatprotec.2006.05.013>.
11. Hassan A M. The effects of ball and roller burnishing on the surface roughness and hardness of some non-ferrous metals. *Journal of Materials Processing Technology* 1997; 72: 385-391, [https://doi.org/10.1016/S0924-0136\(97\)00199-4](https://doi.org/10.1016/S0924-0136(97)00199-4).
12. Janczewski Ł, Tobiła D, Brostow W, Czechowski K, Hagg Lobland K E, Kot M, Zagórski K. Effects of ball burnishing on surface properties of low density polyethylene. *Tribology International* 2016; 93: 36-42, <https://doi.org/10.1016/j.triboint.2015.09.006>.
13. Jedliński R. Diagnostyka w procesie wyceny wartości pojazdów samochodowych i ustalaniu przyczyn oraz następstw uszkodzeń. *Diagnostyka* 2005; 33: 65-70.
14. Jerez-Mesa R, Gomez-Gras G, Travieso-Rodriguez J A. Surface roughness assessment after different strategy patterns of ultrasonic ball burnishing. *Procedia Manufacturing* 2017; 13: 710-717, <https://doi.org/10.1016/j.promfg.2017.09.116>.

15. Jerez-Mesa R, Travieso-Rodríguez J A, Landon Y, Dessein G, Lluma-Fuentes J, Wagner V. Comprehensive analysis of surface integrity modification of ball-end milled Ti-6Al-4V surfaces through vibration-assisted ball burnishing. *Journal of Materials Processing Technology* 2019; 267: 230-240, <https://doi.org/10.1016/j.jmatprotec.2018.12.022>.
16. Korzynski M, Dzierwa A, Pacana A, Cwanek J. Fatigue strength of chromium coated elements and possibility of its improvement with ball peening. *Surface and Coatings Technology* 2009; 204: 615-620, <https://doi.org/10.1016/j.surfcoat.2009.08.049>.
17. Kovács Z F, Viharos Z J, Kodácsy J. Determination of the working gap and optimal machining parameters for magnetic assisted ball burnishing. *Measurement* 2018; 118: 172-180, <https://doi.org/10.1016/j.measurement.2018.01.033>.
18. Low K O, Wong K J. Influence of ball burnishing on surface quality and tribological characteristics of polymers under dry sliding conditions. *Tribology International* 2011; 44: 144-153. <https://doi.org/10.1016/j.triboint.2010.10.005>
19. Niemczewska-Wojcik M. Wear mechanisms and surface topography of artificial hip joint components at the subsequent stages of tribological tests. *Measurement* 2017; 107: 89-98, <https://doi.org/10.1016/j.measurement.2017.04.045>.
20. PN-EN ISO 25178-2:2012 Geometrical Product Specifications (GPS) - Surface texture: Areal - Part 2: Terms, definitions and surface texture parameters.
21. PN-EN ISO 4516:2004 Powłoki metalowe i inne nieorganiczne. Badania mikrotwardości metodą Vickersa i Knoopa.
22. Priyadarsini Ch, Venkata Ramana V S N, Aruna Prabha K, Swethaa S. A review on ball, roller, low plasticity burnishing process. *Materials Today: Proceedings* 2019; 18(7): 5087-5099, <https://doi.org/10.1016/j.matpr.2019.07.505>.
23. Pu Y, Zhao Y, Zhang H, Zhao G, Meng J, Song P. Study on the three-dimensional topography of the machined surface in laser-assisted machining of Si<sub>3</sub>N<sub>4</sub> ceramics under different material removal modes. *Ceramics International* 2019; In press, Available online 14 November 2019, <https://doi.org/10.1016/j.ceramint.2019.11.017>.
24. Rao D S, Suresh H H, Komaraiah M, Kempaiah U N. Investigations on the effect of ball burnishing parameters on surface hardness and wear resistance of HSLA dual-phase steels. *Materials and Manufacturing Processes* 2008; 23: 295-302, <https://doi.org/10.1080/10426910801937306>.
25. Revankar G D, Shetty R, Rao S S, Gaitonde V N. Analysis of surface roughness and hardness in ball burnishing of titanium alloy. *Measurement* 2014; 58: 256-268, <https://doi.org/10.1016/j.measurement.2014.08.043>.
26. Revankar G D, Shetty R, Rao S S, Gaitonde V N. Wear resistance enhancement of titanium alloy (Ti-6Al-4V) by ball burnishing process. *Journal of Materials Research and Technology* 2017; 6: 13-32, <https://doi.org/10.1016/j.jmrt.2016.03.007>.
27. Sadowski Ł, Czarnecki S, Hoła J. Evaluation of the height 3D roughness parameters of concrete substrate and the adhesion to epoxy resin. *International Journal of Adhesion and Adhesives* 2016; 67: 3-13, <https://doi.org/10.1016/j.ijadhadh.2015.12.019>.
28. Saldaña-Robles A, Plascencia-Mora H, Aguilera-Gómez E, Saldaña-Robles A, Marquez-Herrera A, Diosdado-De la Peña J A. Influence of ball-burnishing on roughness, hardness and corrosion resistance of AISI 1045 steel. *Surface and Coatings Technology* 2018; 339: 191-198, <https://doi.org/10.1016/j.surfcoat.2018.02.013>.
29. Sedlacek M, Podgornik B, Vizintin J. Influence of surface preparation on roughness parameters, friction and wear. *Wear* 2009; 266: 482-487, <https://doi.org/10.1016/j.wear.2008.04.017>.
30. Swirad S, Wdowik R. Determining the effect of ball burnishing parameters on surface roughness using the Taguchi method. *Procedia Manufacturing* 2019; 34: 287-292, <https://doi.org/10.1016/j.promfg.2019.06.152>.
31. Swirad S, Wydrzynski D, Nieslony P, Krolczyk G M. Influence of hydrostatic burnishing strategy on the surface topography of martensitic steel. *Measurement* 2019; 138: 590-601, <https://doi.org/10.1016/j.measurement.2019.02.081>.
32. Teimouri R, Amini S, Bagheri Bami A. Evaluation of optimized surface properties and residual stress in ultrasonic assisted ball burnishing of AA6061-T6. *Measurement* 2018; 116: 129-139, <https://doi.org/10.1016/j.measurement.2017.11.001>.
33. Travieso-Rodríguez J A, Jerez-Mesa R, Gómez-Gras G, Lluma-Fuentes J, Casadesús-Farràs O, Madueño-Guerrero M. Hardening effect and fatigue behavior enhancement through ball burnishing on AISI 1038. *Journal of Materials Research and Technology* 2019, 8(6): 5639-5646, <https://doi.org/10.1016/j.jmrt.2019.09.032>.
34. Valiorgue F, Zmelty V, Dumas M, Chomienne V, Verdu C, Lefebvre F, Rech J. Influence of residual stress profile and surface microstructure on fatigue life of a 15-5PH. *Procedia Engineering* 2018; 213: 623-629, <https://doi.org/10.1016/j.proeng.2018.02.058>.
35. Yilmaz H, Sadeler R. Impact wear behavior of ball burnished 316L stainless steel. *Surface and Coatings Technology* 2019; 363: 369-378, <https://doi.org/10.1016/j.surfcoat.2019.02.022>.
36. Zaleski K. The effect of vibratory and rotational shot peening and wear on fatigue life of steel. *Eksplotacja i Niezawodność - Maintenance and Reliability* 2017; 19(1): 102-107, <https://doi.org/10.17531/ein.2017.1.14>.
37. Zhang P, Liu Z. Enhancing surface integrity and corrosion resistance of laser clad Cr-Ni alloys by hard turning and low plasticity burnishing. *Applied Surface Science* 2017; 409: 169-178, <https://doi.org/10.1016/j.apsusc.2017.03.028>.
38. Żurowski W. Structural factors contributing to increased wear resistance of steel friction couples. *Eksplotacja i Niezawodność - Maintenance and Reliability* 2012; 14(1): 19-23.
39. Żurowski W, Brzózka K, Górka B. Analysis of surface layers and wear products by Mössbauer spectral analysis. *Wear* 2013; 297(1): 958-965, <https://doi.org/10.1016/j.wear.2012.10.012>.
40. Żurowski W, Brzózka K, Górka B. Structure of friction products and the surface of tribological system elements. *Nukleonika* 2013; 58: 99-103.

---

**Andrzej DZIERWA**

**Lidia GAŁDA**

Rzeszow University of Technology  
Faculty of Mechanical Engineering and Aeronautics  
ul. Powstańców Warszawy 8, 35-959 Rzeszow, Poland

**Mirosław TUPAJ**

Rzeszow University of Technology  
Faculty of Mechanics and Technology  
ul. Kwiatkowskiego 4, 37-450 Stalowa Wola, Poland

**Kazimiera DUDEK**

University of Rzeszow  
Centre for Innovative Technologies,  
ul. Pigońia 1, 35-310 Rzeszow, Poland

E-mails: [adzierwa@prz.edu.pl](mailto:adzierwa@prz.edu.pl), [lgktmiop@prz.edu.pl](mailto:lgktmiop@prz.edu.pl),  
[mirek@prz.edu.pl](mailto:mirek@prz.edu.pl), [kaziadudek@o2.pl](mailto:kaziadudek@o2.pl)

---